

Safety-oriented CFD analysis of the PeLUIt-40 pebble-bed HTGR under partial flow and LOCA scenarios

Muhammad Thowil Afif¹, Farisy Yogatama Sulisty¹, Dmitriy G. Veretennikov²

¹ *Research Center for Nuclear Reactor Technology, Research Organization for Nuclear Energy, National Research and Innovation Agency of Indonesia, Tangerang Selatan, 15310, Indonesia*

² *National Research, Tomsk Polytechnic University, 30 Lenin Ave., 634050 Tomsk, Russia*

Corresponding author: Muhammad Thowil Afif (muha216@brin.go.id)

Academic editor: Yury Korovin ♦ **Received** 30 September 2025 ♦ **Accepted** 28 January 2026 ♦ **Published** 9 March 2026

Citation: Afif MT, Sulisty FY, Veretennikov DG (2026) Safety-oriented CFD analysis of the PeLUIt-40 pebble-bed HTGR under partial flow and LOCA scenarios. *Nuclear Energy and Technology* 12(1): 19–28. <https://doi.org/10.3897/nucet.12.173615>

Abstract

In this study, the thermal–hydraulic behavior of the Indonesian Micro Reactor PeLUIt-40, a 40 MWt modular pebble-bed high-temperature gas-cooled reactor (HTGR), was analyzed under reduced coolant flow and loss-of-coolant accident (LOCA) conditions. Three-dimensional computational fluid dynamics (CFD) simulations using a porous-media core model and volumetric heat sources from neutronic analysis were performed. Steady-state simulations were conducted for helium flow rates from 100% to 25% of nominal, and a transient LOCA was simulated by reducing flow to zero over ten seconds. The results show that maximum core temperatures increased nonlinearly with reduced flow, exceeding TRISO fuel limits at 25% flow, while outlet duct temperatures remained well homogenized. During the LOCA, passive buoyancy-driven circulation limited temperature rise, stabilizing around 1026 °C. These findings provide preliminary insight into PeLUIt-40 thermal hydraulics, highlighting the need for further validation and extended transient analysis to confirm safety margins.

Keywords

CFD, HTGR, loss-of-coolant accident, PeLUIt-40, safety analysis, thermal hydraulics

Introduction

High-Temperature Gas-cooled Reactors (HTGRs) are widely recognized as one of the most promising candidates in the Generation IV reactor portfolio. Their inherent safety characteristics, high thermal efficiency, and the ability to deliver outlet helium temperatures above 700 °C make them attractive not only for electricity production but also for cogeneration applications such as hydrogen generation, process heat supply, and seawater desalination (Nian 2018; Sato and Yan 2019; Sato et al. 2020).

The combination of TRISO-coated particle fuel, graphite moderator, and helium coolant provides HTGRs with

exceptional safety margins, as these features ensure fission product retention and eliminate the risk of core meltdown even under abnormal conditions (García-Berrocal and Montalvo 2015; Purba and Tjahyani 2019; Chen et al. 2025). These attributes have driven extensive international development. In China, the 10 MWt HTR-10 achieved criticality in 2000, and its successful operation paved the way for the construction of the 200 MWe HTR-PM commercial demonstration plant at Shidao Bay (Zhang et al. 2016; Wu et al. 2002). Other notable designs include South Africa's PBMR-400 and the GT-MHR by General Atomics, all of which reflect the technological maturity and global relevance of HTGR systems (IAEA 2013).

Recent thermal–hydraulic studies have emphasized the importance of coolant-flow management for HTGR safety. For example, Zhang et al. (2021) showed through three-dimensional CFD simulations of the HTR-PM that even partial reductions in helium mass flow can produce substantial increases in core and outlet temperatures. Consistent with these findings, the present study demonstrates a clear steady-state sensitivity of the PeLUIt-40 thermal response to flow degradation. When the inlet mass flow decreases from 17.08 kg/s (100%) to 8.54 kg/s (50%), the maximum core temperature rises from 787.8 °C to 1324.8 °C, corresponding to a 68% increase. The outlet temperature exhibits a comparable behaviour: the average outlet value increases by 64.2%, and the maximum outlet temperature by 64.3%. These steady-state results confirm that even moderate reductions in forced convection can markedly elevate thermal loads in pebble-bed HTGRs. Natural convection provides some degree of passive removal, but the maximum core temperature remains the dominant parameter for fuel integrity. Consequently, each HTGR design requires dedicated thermal–hydraulic evaluation to ensure robust performance under both normal and degraded-flow conditions.

In this context, Indonesia has introduced the Indonesian Micro Reactor (IMR) PeLUIt-40, a 40 MWt modular pebble-bed HTGR intended for cogeneration application (Setiadipura et al. 2021; Trianti et al. 2023; Wisnubroto et al. 2023; Dewita et al. 2024). The reactor employs helium coolant at 3.0 MPa, operating between 250 °C at the inlet and about 700 °C at the outlet, with a dedicated hot gas chamber that homogenizes outlet flow before it enters four ducts connected to the steam generator. While the compact configuration is designed to balance efficiency and safety, its novel geometry and relatively small power rating distinguish it from international counterparts such as HTR-PM. This difference necessitates safety-oriented thermal–hydraulic assessments tailored specifically to PeLUIt-40, particularly regarding reduced coolant flow and accident transients.

The objectives of this study are threefold. First, to quantify the maximum fuel temperature of PeLUIt-40 under steady-state conditions with reduced coolant flow, thereby identifying the safety margins relative to the TRISO failure threshold. Second, to evaluate outlet helium uniformity across different flow conditions, with particular emphasis on the performance of the hot gas chamber in mitigating temperature gradients. Third, to analyze the transient thermal–hydraulic response during a rapid LOCA, including the role of buoyancy-driven passive cooling in redistributing heat once forced convection is lost. Together, these investigations provide a safety-oriented perspective on the thermal–hydraulic behavior of PeLUIt-40, contributing to its future deployment and regulatory assessment as Indonesia’s first modular HTGR for cogeneration applications.

Materials and methods

Design characteristics of the PeLUIt-40 and relevance for safety analysis

The Indonesian Micro Reactor PeLUIt-40 is a 40 MWt modular pebble-bed HTGR developed to supply both electricity and heat for industrial processes. Its design adopts helium as the primary coolant and graphite as moderator, combining a chemically inert working fluid with excellent high-temperature stability. Operating at a system pressure of 3.0 MPa, helium enters the reactor at 250 °C and leaves the core at around 700 °C, providing a temperature rise sufficient for cogeneration and hydrogen production. These parameters place PeLUIt-40 within the operating envelope of other Generation IV pebble-bed concepts, while keeping the design compact for deployment in remote or industrial regions.

The core contains roughly 27000 spherical fuel pebbles arranged in a random packing. Each pebble consists of TRISO fuel particles embedded in a graphite matrix, ensuring fission product retention and thermal robustness. The cylindrical core has a diameter of about 1.8 m and an effective height of 1.97 m, yielding a power density suitable for long operating cycles. The random pebble arrangement creates an interconnected porous structure that enables helium to flow through the interstitial channels and extract heat efficiently (Trianti et al. 2023; Miftasani et al. 2024, 2025).

At the lower boundary of the core, the conical fuel discharge channel fulfills a dual role. During normal operation, it guides spent pebbles toward the refueling system, while at the same time acting as a passage for heated helium to exit the core and enter the plenum. This configuration is shown in Fig. 1 and it integrates fuel management with coolant circulation, an inherent feature of pebble-bed reactor technology.

To mitigate the uneven temperature distribution that arises from higher neutron flux at the core center, PeLUIt-40 employs a two-stage coolant mixing system. First, the bottom plenum collects and partially blends helium streams leaving different radial zones of the core. The flow then enters a larger hot gas chamber located beneath the reactor vessel, where thorough mixing occurs before the coolant is routed toward the steam generator. This arrangement significantly reduces axial and radial temperature gradients, thereby minimizing thermal stresses on downstream components.

The homogenized helium is subsequently directed through four outlet ducts that connect the reactor pressure vessel to the heat-exchanger system. Using multiple ducts rather than a single large channel provides two main advantages: the flow is more evenly distributed across the steam generator modules, and localized hot spots are avoided. Together, the hot gas chamber and multi-duct system form a critical part of the thermal-hydraulic safety

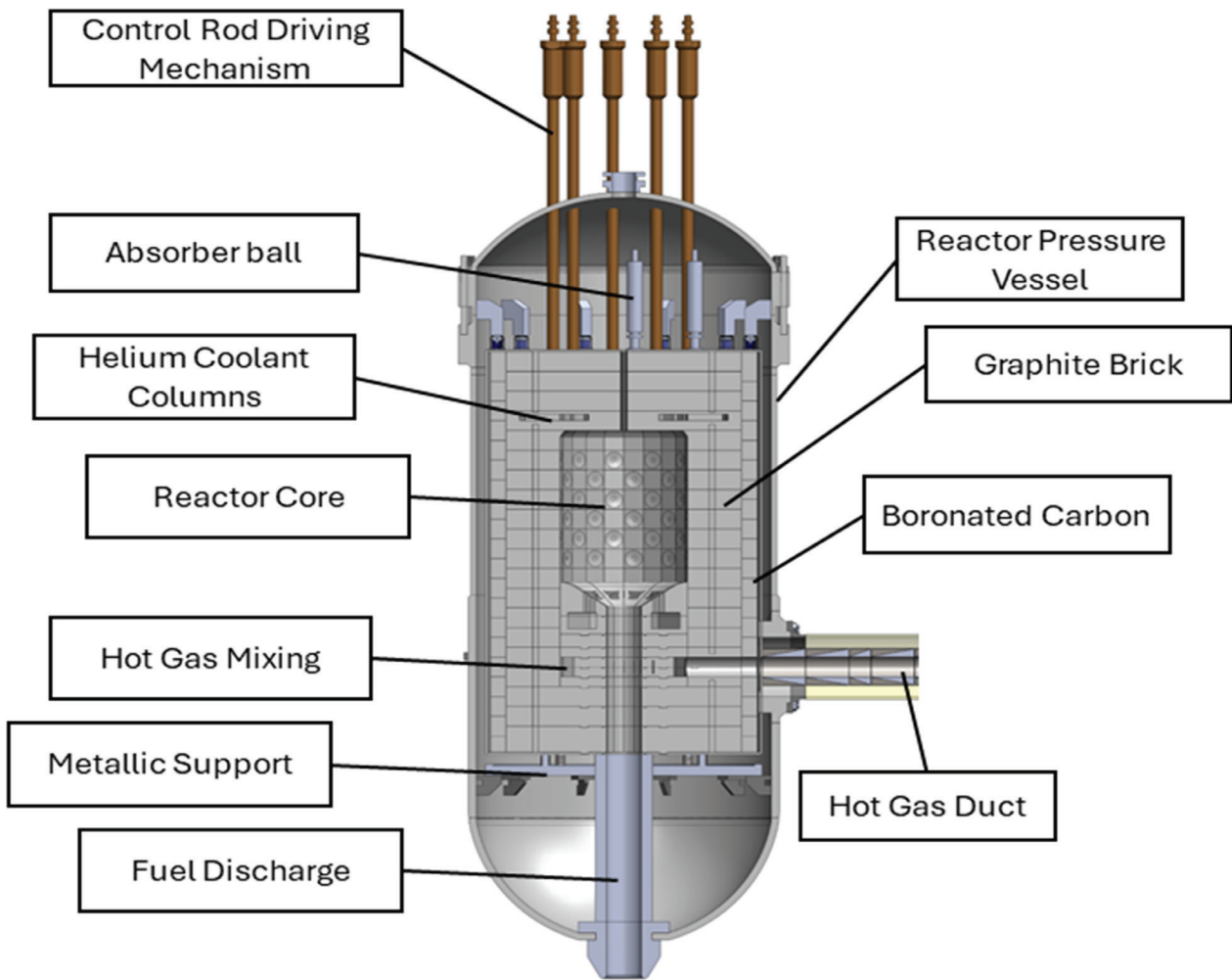


Figure 1. Configuration of the PeLUIt 40MWth Vessel (IAEA 2024).

strategy of PeLUIt-40, ensuring both efficient energy transfer and long-term structural integrity of the primary circuit (Dwijayanto et al. 2019; Dewita et al. 2024).

Numerical methodology

The thermal–hydraulic behavior of the PeLUIt-40 was studied using three-dimensional CFD simulations in ANSYS Fluent (Dwijayanto et al. 2019; ANSYS 2021; Huning et al. 2021). The computational domain extended from the helium inlet through the porous pebble-bed core and discharge channel, into the bottom plenum and hot gas chamber, and finally through four outlet ducts connected to the steam-generator system as shown in Fig. 2.

The governing equations solved were the Reynolds-averaged continuity, momentum, and energy equations. Additional momentum-sink terms were applied within the porous regions, and volumetric heat-source terms were used to represent heat generation in the fuel compacts. Turbulence closure employed the Standard $k-\epsilon$ model with standard wall functions, a formulation widely used and validated in high-temperature gas-cooled reactor analyses (Versteeg and Malalasekera 2007). A pres-

sure-based finite-volume solver with second-order spatial discretization was applied.

Helium was modeled as a compressible coolant with temperature-dependent density, viscosity, specific heat, and thermal conductivity, implemented through established correlations covering the reactor’s operating range. Under nominal conditions, the system pressure is 3.0 MPa, the mass flow rate is 17.08 kg/s, and the coolant enters the core at approximately 250 °C with a design outlet temperature of around 700 °C.

To justify the choice of turbulence model, additional simulations were performed using RNG $k-\epsilon$, Realizable $k-\epsilon$, and SST $k-\omega$ models. All models produced nearly identical core and outlet temperatures (variation <1 °C), indicating that the global flow and heat-transfer behavior in the reactor are not strongly sensitive to the turbulence formulation. The inlet Reynolds number is on the order of 10^5 under nominal flow conditions, which lies within the recommended applicability range of the Standard $k-\epsilon$ model.

Because the core, bottom plenum, and hot gas chamber contain porous-media regions, the near-wall flow is dominated by volumetric drag rather than classical wall-bound shear layers. Consequently, the y^+ values obtained on

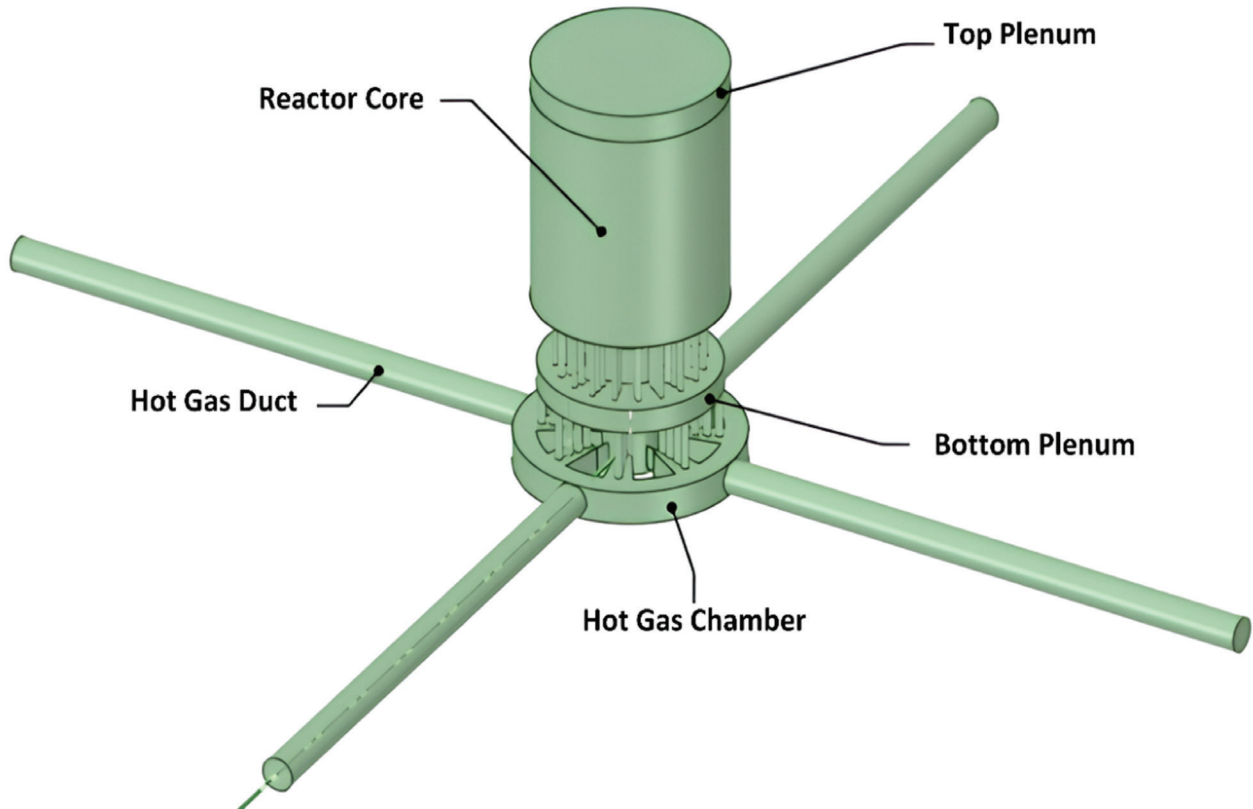


Figure 2. Simplified fluid domain of PeLUIt-40 including core, plenum, hot gas chamber, and Hot gas outlet ducts.

solid walls are significantly higher than those characteristic of smooth-wall channel flows. Sensitivity tests with different boundary-layer mesh refinements (3–18 inflation layers) showed negligible changes in predicted temperatures, confirming that the solution is governed primarily by bulk mixing and porous-media resistance rather than near-wall resolution. For these reasons, the Standard $k-\epsilon$ model with wall functions was retained for the final simulations.

Table 1. Key CFD model parameters and boundary conditions

Parameter	Value
Working fluid	Helium
System pressure	3.0 MPa
Inlet mass flow	17.08 kg/s
Inlet temperature	250 °C
Turbulence model	$k-\epsilon$, standard wall functions
Porosity	0.39
Viscous resistance	$2.61 \times 10^5 \text{ m}^{-2}$
Inertial resistance	599.9 m^{-1}
Outlet ducts	Four pressure outlets (700 °C backflow)
Gravit	9.81 m/s^2

Core representation

The pebble-bed core, which contains approximately 27,000 spherical fuel elements, was modeled as a homogeneous and isotropic porous medium to avoid the prohibitive computational cost of explicitly resolving each pebble. Flow resistance within the porous zone was applied through Darcy–Forchheimer momentum-sink terms. The viscous and inertial resistance coefficients ($2.61 \times 10^5 \text{ m}^{-2}$

and 599.9 m^{-1} , respectively) were derived from correlations for the pebble diameter and packing fraction and calibrated to match the expected core pressure drop and outlet temperature under nominal helium flow conditions (17.08 kg/s, 3.0 MPa). This approach ensures a physically meaningful representation of pressure losses while remaining consistent with standard HTGR CFD modeling practices in the absence of full-scale experimental data. A porosity of 0.39 was assumed.

Volumetric heat sources (W/m^3) were imposed only in the energy equation according to zone power densities obtained from neutronic analysis. The heat source was defined as piecewise constant in radial and axial zones to capture flux peaking and realistic thermal gradients. These source terms are independent of the momentum equation. For transient LOCA simulations, the helium mass flow is reduced linearly from the nominal 17.08 kg/s to zero over 10 s via a user-defined function, while the volumetric heat generation in the fuel compacts is assumed constant, representing a conservative un-scrammed accident scenario. This formulation ensures a physically meaningful transient thermal response while maintaining numerical stability.

The non-uniform volumetric heat distribution applied to the core is shown schematically in Fig. 3, with representative values listed in Table 2.

Table 2. Representative values volumetric power density (Q) in the core at $z = 1.97 \text{ m}$

$r, \text{ m}$	0.21	0.42	0.63	0.78	0.84	0.90
$Q, \text{ W/m}^3$	$9.58 \cdot 10^6$	$9.07 \cdot 10^6$	$8.21 \cdot 10^6$	$7.46 \cdot 10^6$	$7.29 \cdot 10^6$	$7.42 \cdot 10^6$

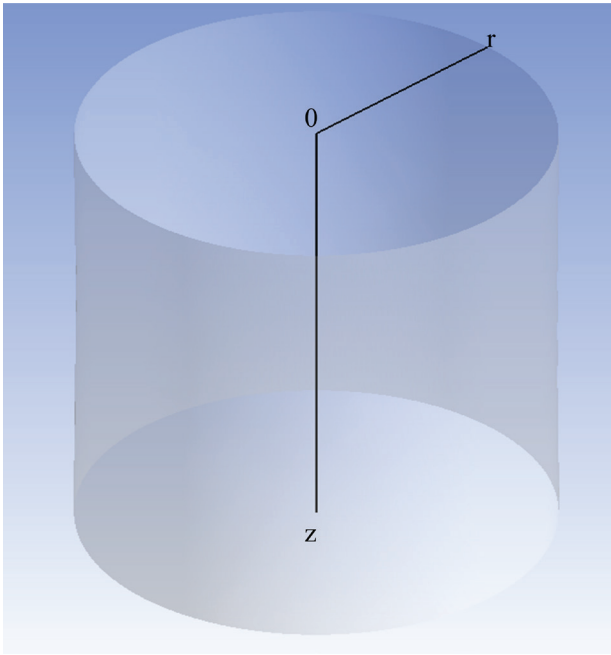


Figure 3. Cylindrical coordinate framework used for zonal mapping of the core power distribution.

Simulation setup and meshing

Both steady and transient cases were analyzed. In steady state, five inlet mass-flow conditions were imposed: 100%, 90%, 75%, 50%, and 25% of the nominal flow. The inlet helium temperature was kept at 250 °C and the system pressure at 3 MPa. Each of the four outlet ducts was modeled as a pressure outlet, with a backflow temperature of 700 °C specified to ensure numerical stability.

All walls were treated as adiabatic. These steady simulations represented normal operation at design conditions as well as partial flow-reduction scenarios, such as pump degradation or channel blockage.

The transient scenario modeled a rapid depressurization (LOCA). The simulation was initialized from the converged 100% steady case. The inlet mass flow was reduced linearly from 17.08 kg/s to zero over 10 s, after which the calculation was continued for an additional 50 s under zero-flow boundary conditions. This setup captured the buoyancy-driven redistribution of helium in the vessel following coolant loss. The SIMPLE algorithm was applied, with a fixed time step of 0.01 s and 20 iterations per step; other solver parameters were left at their Fluent defaults. Convergence criteria required residuals below 10^{-3} for continuity and momentum, and 10^{-6} for energy, in addition to stabilization of integral quantities such as maximum core temperature. An a-posteriori check of the convective Courant number showed an area-weighted average value of 0.165 across the domain, indicating that the chosen time step provided sufficient temporal resolution for the transient calculations.

The geometry was discretized using a poly-hexcore grid as shown in Figs 4, 5. This hybrid strategy combined structured hexahedral layers in simpler regions with unstructured polyhedral cells in more complex sections, such as the hot gas chamber. Refinement was applied at the core-plenum interface, within the hot gas chamber, and around the duct inlets to accurately capture flow redistribution and mixing. The final grid contained 646415 cells. Quality metrics indicated a maximum skewness of 0.7 and a minimum orthogonality of 0.15, both within the recommended range for reactor-scale CFD (Versteeg and Malalasekera 2007).

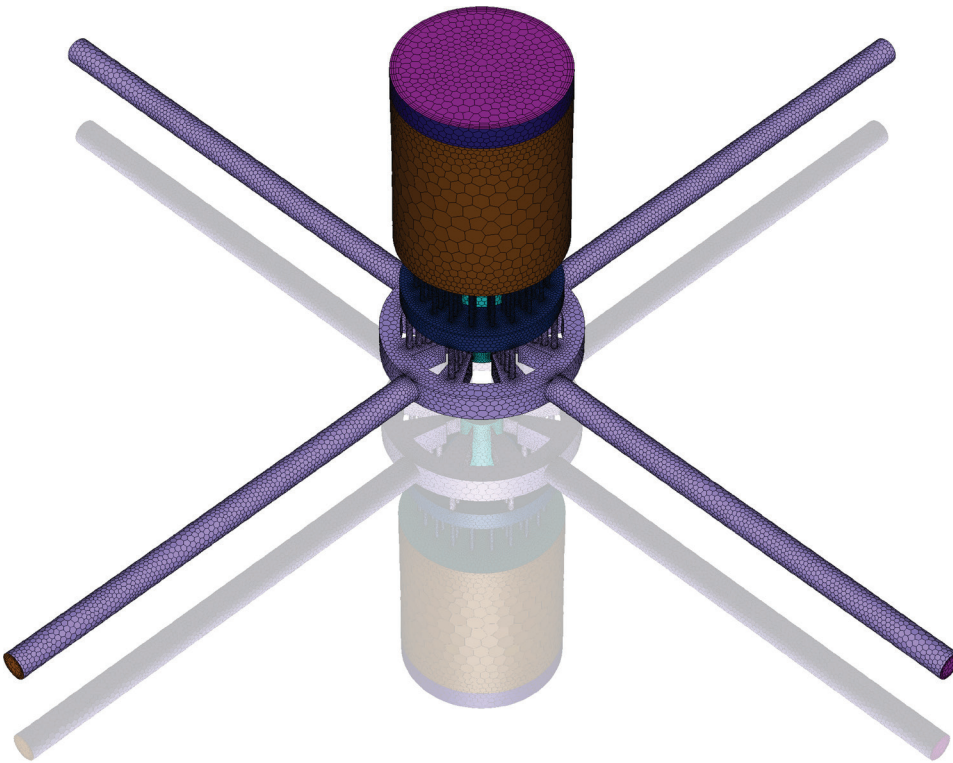


Figure 4. Mesh of the PeLUit-40 fluid domain.

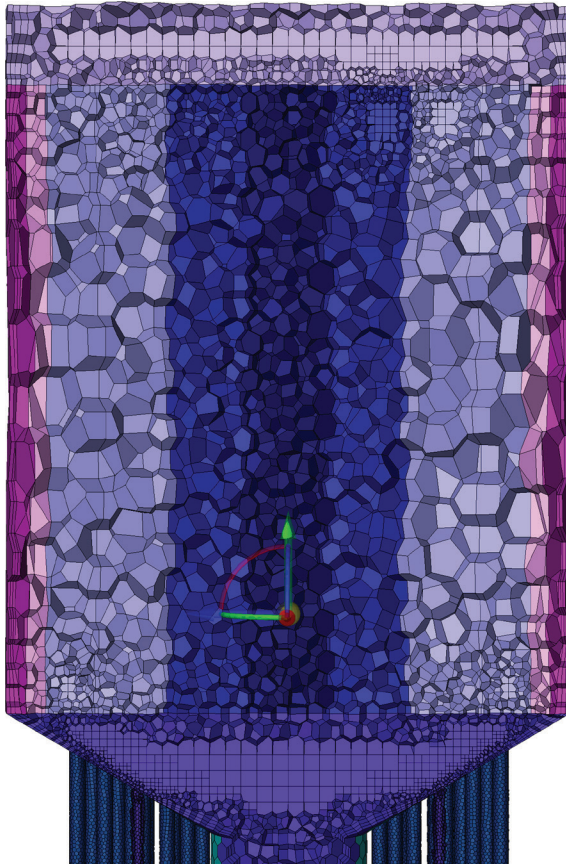


Figure 5. Volume mesh cut section at the reactor core region using Poly-hexcore.

A dedicated mesh-independence study was carried out under steady-state conditions at 90% nominal mass flow (15.372 kg/s), selected as a representative operating point with elevated thermal gradients while remaining within the safe envelope. Three mesh configurations – coarse (529,750 cells), average (646,415 cells), and fine (1,023,402 cells) – were evaluated. The results, summarized in Table 3, show negligible variation in key thermal metrics: the maximum core temperature differed by less than 0.3 °C, and outlet duct temperatures varied by less than 1 °C across meshes. These findings confirm that the adopted mesh resolution is sufficient to capture the global thermal–hydraulic behavior of the reactor, including mixing in the hot gas chamber, which is critical for both steady-state and transient LOCA scenarios. Mesh quality metrics (maximum skewness < 0.7, minimum orthogonality > 0.15) satisfied accepted CFD best-practice criteria (IAEA 2003; NEA/CSNI 2024). The selected mesh resolution (646,415 cells) therefore provides a reliable balance between computational efficiency and accuracy, ensuring robust predictions for the safety-focused objectives of this study (Dwijayanto et al. 2019; ANSYS 2021). Future studies may consider symmetry-based domain re-

duction to further optimize computational cost, particularly for extended parametric sensitivity analyses.

Results and discussion

The CFD simulations provided comprehensive insights into the thermal–hydraulic behavior of the PeLUit-40 under steady-state and transient conditions. Two key safety-related indicators were emphasized: the maximum temperature in the porous core, which determines the thermal margin of the TRISO fuel, and the uniformity of outlet temperatures among the four hot gas ducts, which reflects the effectiveness of the hot gas chamber in homogenizing the coolant before entering downstream components.

Steady-state thermal behavior

The reactor was first analyzed under steady-state operation at five different inlet helium mass flow rates. Table 3 summarizes the key results, including the maximum porous-core temperature, the average outlet temperature across the ducts, and the maximum duct outlet temperature.

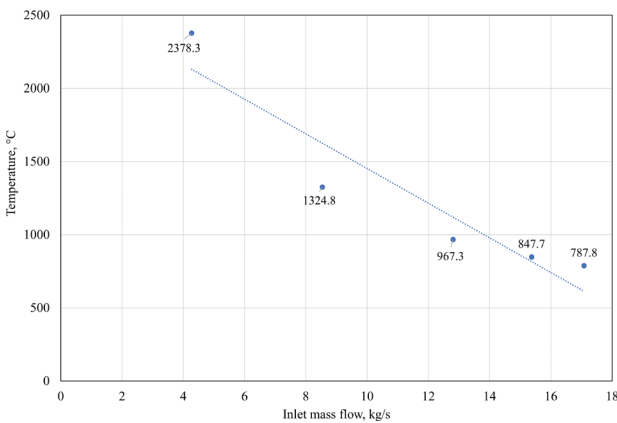
Table 3. Mesh sensitivity analysis at 90% nominal flow (15.372 kg/s)

Number of cells	Number of nodes	Max core temperature, °C	Average outlet duct temperature, °C	Max outlet duct temperature, °C
529750	1747877	847.94	747.94	748.79
646415	2072397	847.70	747.90	749.70
1023402	3225132	847.83	747.95	748.98

Table 4. Steady-state thermal performance at different coolant flow rates

Inlet mass flow, kg/s	Relative flow, %	Max core temperature, °C	Average outlet duct temperature, °C	Max outlet duct temperature, °C
17.08	100	787.8	698.2	700.2
15.37	90	847.7	747.0	749.7
12.81	75	967.3	847.5	849.6
8.54	50	1324.8	1146.31	1149.9
4.27	25	2378.3	2042.6	2048.6

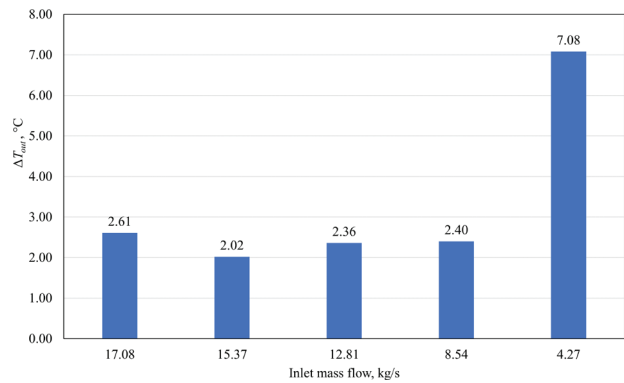
As shown in Fig. 6, at nominal coolant flow, the maximum porous-core temperature reached approximately 788 °C. Analytical estimation of radial heat conduction within the 6 cm diameter graphite pebbles suggests that the peak fuel kernel temperature is approximately 118 °C higher than the porous average. Even with this correction, the fuel temperature remains well below the TRISO particle failure threshold of 1500–1600 °C. This indicated that under design conditions, PeLUIt-40 operated with substantial safety margins. As coolant flow was reduced, a clear nonlinear rise in core temperature was observed. At 75% of nominal flow, the maximum core temperature approached 970 °C, still within the acceptable envelope but with a noticeably reduced margin. At 50% flow, the maximum porous temperature reached approximately 1325 °C. When accounting for the internal conduction factor, the peak fuel temperature is estimated to reach approximately 1443 °C which remained technically below the TRISO limit but already encroached on critical margins defined for HTGRs in international benchmarks (Zhang et al. 2021; Miftasani et al. 2025).

**Figure 6.** Maximum porous-core temperature as a function of inlet helium flow rate.

A severe temperature excursion occurred at 25% flow, with the core exceeding 2370 °C – well beyond the TRISO failure limit – indicating that such conditions would lead to fuel coating degradation and loss of integrity. This scenario was conducted as a parametric study to define the ultimate safety envelope of the core under hypothetical failure conditions (e.g., failure to SCRAM), rather than standard operating procedures. (Sato and Yan 2019; Dewita et al. 2024).

In parallel with the core analysis, the outlet temperature uniformity across the four ducts was evaluated based

on the area-averaged temperature at each duct outlet, as shown in Fig. 7. The uniformity metric was defined as the duct-to-duct temperature deviation, calculated as the difference between the highest and lowest area-averaged outlet temperatures ($\Delta T_{\text{uniformity}} = \max(T_i) - \min(T_i)$). At nominal flow, this deviation remained below 3 °C, indicating an effective mixing performance within the hot-gas chamber. Even at reduced inlet flow, homogenization remained strong, with duct-to-duct deviation below 7 °C at the most extreme 25%-flow condition. These findings demonstrate that the PeLUIt-40 outlet chamber effectively minimizes thermal non-uniformities, thereby limiting cyclic thermal stresses on downstream components such as the steam generator (Dwijayanto et al. 2019; Miftasani et al. 2024). The resulting uniform helium temperature distribution contributes to improved overall system reliability during long-term operation.

**Figure 7.** Outlet duct temperatures and ΔT_{out} as a function of inlet helium flow rate.

Transient LOCA response

A rapid depressurization accident was simulated by reducing the helium inlet mass flow from 17.08 kg/s to zero over 10 s, followed by 50 s of zero-flow conditions. The resulting time evolution of maximum porous-core temperature was analyzed and is presented in Fig. 8.

As the inlet flow decreased, the core temperature rose rapidly due to diminished forced convection. After complete loss of flow at $t = 10$ s, the rate of temperature rise briefly slowed during the 10–20 s interval, as limited buoyancy-driven recirculation began to form initial natural-convection pathways.

The maximum temperature reached approximately 1026 °C at the end of the early transient phase, corresponding to a Figure of Merit (FoM) 50% above the nominal

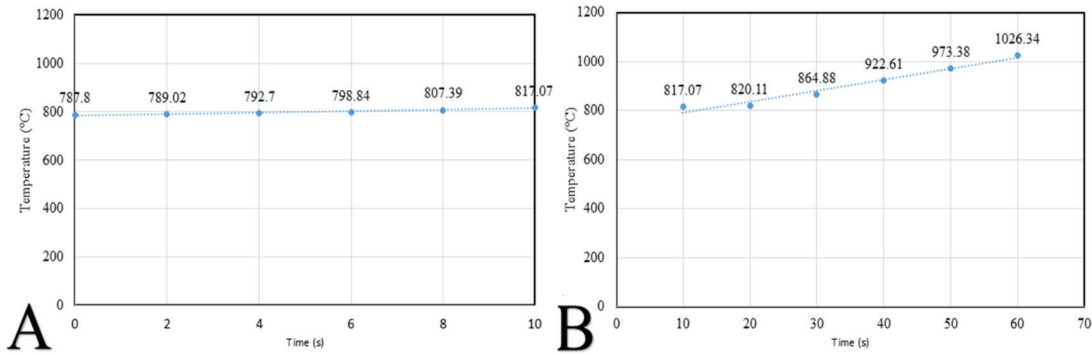


Figure 8. Time evolution of maximum porous-core temperature. **A.** During LOCA; **B.** After no inlet coolant.

design limit, while remaining below the value observed in the extreme 25% steady-state case. This temperature does not represent a stabilized maximum, and under sustained coolant loss without SCRAM or neglecting radiative heat transfer, the temperature would continue to rise.

After the helium inlet was lost at $t = 10$ s, the core temperature continued to rise. Between 10–20 s, the temperature increase was 3.04 °C, reflecting the early post-loss period in which residual cooling and the delayed thermal response still moderated the core heating rate. During 20–30 s and 30–40 s, heating accelerated significantly, with predicted increments of 44.8 °C and 57.7 °C, respectively, due to the dominance of volumetric heating and limited natural convection. For the next intervals (40–50 s and 50–60 s), the temperature rise was estimated at 5.3 °C per 10 s, based on the calculated rate of temperature change.

The rate of temperature rise (dT/dt) for each interval, shown in Fig. 9, indicates the periods during which thermal management or emergency action would be most critical during the LOCA transient. In this study, the Figure-of-Merit (FoM) was defined as the temperature increment over each 10-s interval after helium flow reached zero, computed using $FoM = \Delta T/\Delta t$. Based on the six consecutive intervals between 0 and 60 s, the calculated FoM values yielded an average temperature increase of 26.98 °C per 10 s. This averaged value provides a practical indicator of the core's thermal escalation rate during extended coolant-loss conditions. Although this trend suggests rapid temperature growth under sustained flow absence, it remains a conservative estimate because potential mitigating effects such as natural convection and

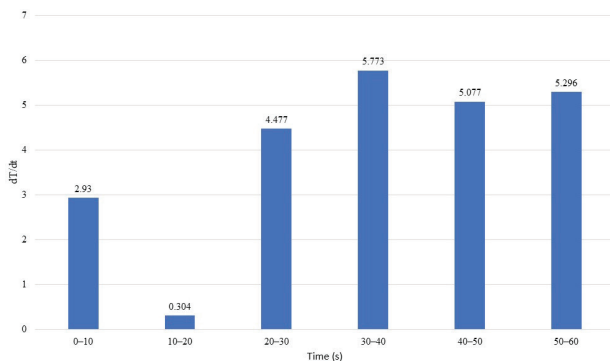


Figure 9. Maximum core temperature and its temporal gradient (dT/dt) over time.

radiative heat transfer were not included (Dwijayanto et al. 2019; Huning et al. 2021).

These results emphasize both the early-stage effects of residual cooling and the later-stage acceleration of heating, offering quantitative guidance for emergency planning and the evaluation of thermal safety margins in the porous-core design.

The spatial temperature field at the end of the transient ($t = 60$ s) is shown in Fig. 10. The hottest region is located at the lower part of the porous core, corresponding to the coolant outlet path, where reduced convective removal coincided with continued volumetric heating.

Safety implications

The results confirmed the inherent thermal–hydraulic resilience of the PeLUIt-40 under a range of operating conditions, but also highlighted critical safety thresholds:

- 1) Under nominal and moderately reduced flow ($\geq 50\%$), thermal margins remained sufficient and outlet homogenization was effective.
- 2) At 25% flow, the local maximum temperature (2378 °C) greatly exceeded the TRISO integrity limit. This indicated that operation at such low coolant flow was not tolerable and must be excluded from the reactor's safe operating envelope (Dewita et al. 2024; Miftasani et al. 2025).
- 3) In the LOCA scenario (0–60 s), the maximum temperature rose steadily, reaching 1026.34 °C at 60 s. As indicated by the temperature rate of change ($\Delta T/dt$ approx 5.3 °C/s at $t=60$ s), the core temperature was still increasing and had not yet reached equilibrium. However, the progression demonstrates the thermal inertia of the core, which mitigates rapid temperature excursions immediately following the accident initiation (Dwijayanto et al. 2019; Zhang et al. 2021).

Overall, the simulations suggested that while the PeLUIt-40 exhibited strong inherent safety characteristics, a conservative lower bound for operational coolant flow should be defined (no lower than 50% of nominal). Additional design measures, such as enhanced passive cooling channels or increased hot gas chamber volume, could fur-

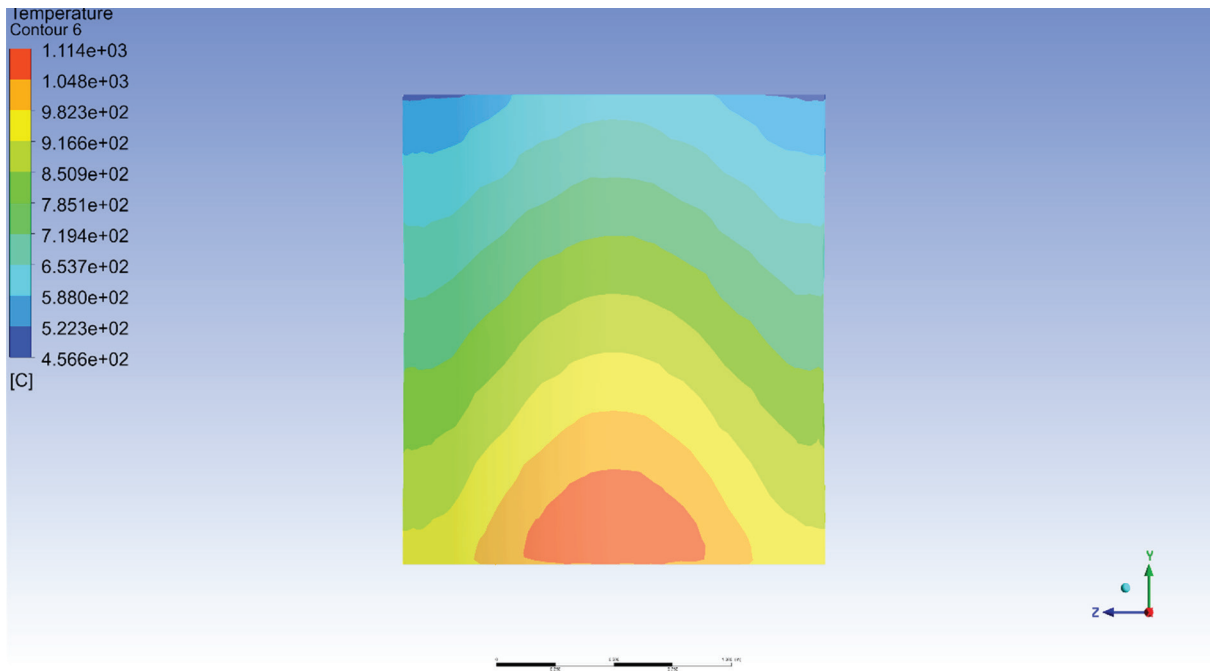


Figure 10. Temperature distribution in the porous core at $t = 60$ s after coolant loss.

ther extend the safety envelope for severe accident scenarios (Setiadipura et al. 2021).

To further mitigate the risk of high core temperatures resulting from significant coolant flow reduction, the reactor is equipped with multiple layers of safety mechanisms. Beyond the primary, immediate SCRAM triggered by the Reactor Protection System (RPS) upon detecting low flow or high temperature, several passive systems are designed to operate. These include the Reactor Cavity Cooling System (RCCS), which passively removes decay heat from the reactor vessel wall via natural convection, transferring heat to the ultimate heat sink. Additionally, a severe temperature or flow anomaly would activate the secondary shutdown mechanism, involving the gravity-driven drop of neutron absorber balls into the core. This diverse safety measure rapidly brings the reactor to a subcritical state, effectively reducing the heat generation rate and ensuring long-term thermal stability.

Conclusion

In this work, the thermal–hydraulic behavior of the Indonesian micro modular reactor PeLUIt-40 was analyzed under steady-state and transient accident conditions using three-dimensional CFD modeling. The porous-medium approximation was employed to represent the pebble-bed core, with non-uniform volumetric heat sources mapped from neutronic data.

The results showed that under nominal operation the reactor maintained large thermal margins, and even with a 50% reduction in coolant flow the maximum core temperature remained below the TRISO integrity limit. At 25% of nominal flow, however, the maximum porous-core temperature rose to approximately 2400 °C, far beyond the

conservative failure threshold of 1500–1600 °C, clearly identifying this regime as outside the safe operating envelope (Sato and Yan 2019; Dewita et al. 2024; Miftasani et al. 2025). Across all steady conditions, the hot gas chamber was effective in homogenizing outlet flows, thereby protecting downstream components from thermal stress (Dwijayanto et al. 2019; Miftasani et al. 2024).

In the rapid depressurization scenario, the maximum temperature increased sharply as forced convection diminished, but the rate of rise slowed once buoyancy-driven natural circulation was established. The temperature stabilized at around 1026.34 °C, confirming the delaying role of passive mechanisms in moderating accident progression (Dwijayanto et al. 2019; Zhang et al. 2021).

Taken together, these findings confirmed that the PeLUIt-40 design exhibits strong inherent safety features characteristic of high-temperature gas-cooled reactors. At the same time, the results highlighted the need to define a conservative operational lower limit of coolant flow, not below 50% of nominal, and to consider design enhancements such as improved passive decay-heat removal to further extend safety margins under beyond-design conditions (Setiadipura et al. 2021).

Acknowledgements

We would like to express our sincere gratitude to Dr. Topan Setiadipura, the Head of the Research Center for Nuclear Reactor Technology, for his valuable guidance and support throughout this research. Additionally, we would like to extend our gratitude to High Performance Computer (HPC) of National Research and Innovation Agency (BRIN) for granting us permission to use the ANSYS Fluent in our calculations.

References

- ANSYS Inc. (2021) Ansys ICEM CFD, Release 2021 R2, User's Manual. ANSYS, Inc., Southpointe, PA.
- Chen Y-X, Wu S-R, Chao J, Chao D-S, Hong J-Y, Liang J-H (2025) Comparison of neutronics performance of various TRISO fuels. *Nuclear Engineering and Design* 432: 113825. <https://doi.org/10.1016/j.nucengdes.2025.113825>
- Dewita E, Suwoto, Zuhair, Sriyono, Purwadi M-D, Ariyanto S, Susilo YSB, Sulistyoy FY (2024) Implementation of thorium-based fuel for Indonesia Micro Reactor (IMR). *Nuclear Engineering and Design* 425: 113334. <https://doi.org/10.1016/j.nucengdes.2024.113334>
- Dwijayanto RAP, Sulistyoy FY, Subekti M (2019) CFD analysis on temperature homogenisation performance in experimental power reactor bottom plenum. In: *AIP Conference Proceedings* 2180(1): 020021. American Institute of Physics Inc. <https://doi.org/10.1063/1.5135530>
- García-Berrocal A, Montalvo C (2015) Temperature transients in TRISO type fuel. *Annals of Nuclear Energy* 76: 172–176. <https://doi.org/10.1016/j.anucene.2014.09.031>
- Huning AJ, Chandrasekaran S, Garimella S (2021) A review of recent advances in HTGR CFD and thermal fluid analysis. *Nuclear Engineering and Design* 373: 111013. <https://doi.org/10.1016/j.nucengdes.2020.111013>
- International Atomic Energy Agency (IAEA) (2003) Use of Computational Fluid Dynamics Codes for Safety Analysis of Nuclear Reactor Systems. IAEA-TECDOC-1379, IAEA, Vienna. https://www-pub.iaea.org/MTCD/Publications/PDF/te_1379_web.pdf
- IAEA [International Atomic Energy Agency] (2013) Evaluation of High Temperature Gas Cooled Reactor Performance: Benchmark Analysis Related to the PBMR-400, PBMM, GT-MHR, HTR-10 and the ASTRA Critical Facility. IAEA-TECDOC-1694, IAEA, Vienna, 688 pp. https://www-pub.iaea.org/MTCD/Publications/PDF/TE-1694_web.pdf
- IAEA [International Atomic Energy Agency] (2024) Small Modular Reactor Technology Catalogue, 2024 Edition. A supplement to the IAEA Advanced Reactors Information System (ARIS). IAEA, Vienna. https://aris.iaea.org/Publications/SMR_catalogue_2024.pdf
- Miftasani F, Andika Putra Dwijayanto R, Abrar G, Widiawati N, Trianti N, Setiadipura T, Irwanto D, Wulandari C, Suud Z (2024) Investigating geometry adjustments for enhanced performance in a PeLUIt-10 MWe pebble bed HTGR with OTTO refueling scheme. *Nuclear Engineering and Design* 422: 113163. <https://doi.org/10.1016/j.nucengdes.2024.113163>
- Miftasani F, Wijaya S, Widiawati N, Hidayati AN, Mulyana D, Wafda H, Purwaningsih A, Al Afghani F, Bayquni MI, Waskita AA, Setiadipura T (2025) Analysis of TRISO failure fraction in PeLUIt reactor with increasing power. *Nuclear Engineering and Design* 432: 113842. <https://doi.org/10.1016/j.nucengdes.2025.113842>
- Nuclear Energy Agency (NEA) / Committee on the Safety of Nuclear Installations (CSNI) (2024) Best Practice Guidelines for the Use of CFD in Nuclear Reactor Safety Applications. NEA/CSNI/R(2022)10, OECD-NEA, Paris. https://www.oecd-nea.org/upload/docs/application/pdf/2025-03/nea_csni_r_2022_10.pdf
- Nian V (2018) Technology perspectives from 1950 to 2100 and policy implications for the global nuclear power industry. *Progress in Nuclear Energy* 105: 83–98. <https://doi.org/10.1016/j.pnucene.2017.12.009>
- Purba JH, Tjahyani DTS (2019) A comparative study on safety design requirements between HTGR and LWR. *Journal of Physics: Conference Series* 1198: 022020. <https://doi.org/10.1088/1742-6596/1198/2/022020>
- Sato H, Yan XL (2019) Study of an HTGR and renewable energy hybrid system for grid stability. *Nuclear Engineering and Design* 343: 178–186. <https://doi.org/10.1016/j.nucengdes.2019.01.010>
- Sato H, Aoki T, Ohashi H, Yan XL (2020) Research and development for safety and licensing of HTGR cogeneration system. *Nuclear Engineering and Design* 360: 110493. <https://doi.org/10.1016/j.nucengdes.2019.110493>
- Setiadipura T, Luthfi W, Bakhri S, Suwoto, Zuhair, Li Z, Sun Y (2021) Optimization of PeLUIt-150 conceptual design. *Journal of Physics: Conference Series* 2048: 012027. <https://doi.org/10.1088/1742-6596/2048/1/012027>
- Trianti N, Widiawati N, Wulandari C, Miftasani F, Rohanda A, Khakim A, Setiadipura T (2023) Optimum power determination and comparison of multi-pass and OTTO fuel management schemes of HTGR-based PeLUIt reactor. *Nuclear Engineering and Design* 415: 112696. <https://doi.org/10.1016/j.nucengdes.2023.112696>
- Versteeg H, Malalasekera W (2007) *An Introduction to Computational Fluid Dynamics: The Finite Volume Method* (2nd Edn.). Pearson Higher Ed, 520 pp.
- Wisnubroto DS, Sunaryo GR, Susilo YSB, Bakhri S, Setiadipura T (2023) Indonesia's experimental power reactor program (RDE). *Nuclear Engineering and Design* 404: 112201. <https://doi.org/10.1016/j.nucengdes.2023.112201>
- Wu Z, Lin D, Zhong D (2002) The design features of the HTR-10. *Nuclear Engineering and Design* 218: 25–32. [https://doi.org/10.1016/S0029-5493\(02\)00182-6](https://doi.org/10.1016/S0029-5493(02)00182-6)
- Zhang Z, Dong Y, Li F, Zhang Z, Wang H, Huang X, Li H, Liu B, Wu X, Wang H, Diao X, Zhang H, Wang J (2016) The Shandong Shidao Bay 200 MWe High-Temperature Gas-Cooled Reactor Pebble-Bed Module (HTR-PM) demonstration power plant: an engineering and technological innovation. *Engineering* 2: 112–118. <https://doi.org/10.1016/j.eng.2016.01.020>
- Zhang S, Li L, Zhang Z, Zhang S (2021) Three-dimensional modeling and loss-of-coolant accident analysis of high temperature gas cooled reactor. *Annals of Nuclear Energy* 150: 107840. <https://doi.org/10.1016/j.anucene.2020.107840>